

# Whole-body biodistribution and radiation dosimetry estimates for the PET dopamine transporter probe $^{18}\text{F}$ -FECNT in non-human primates

Dnyanesh N. Tipre, Masahiro Fujita, Frederick T. Chin, Nicholas Seneca, Douglas Vines, Jehi-San Liow, Victor W. Pike and Robert B. Innis

**Background and aim** 2 $\beta$ -Carbomethoxy-3-(4-chlorophenyl)-8-(2-[ $^{18}\text{F}$ ]fluoroethyl)nortropane ( $^{18}\text{F}$ -FECNT) is a selective radioligand for the in vivo quantification of dopamine transporters by using positron emission tomography. The aim of the current study was to quantify the distribution of radioactivity in three rhesus monkeys after the injection of approximately 185 MBq (5 mCi) of  $^{18}\text{F}$ -FECNT.

**Method** Whole-body images were acquired at 23–30 time points for a total of 220 min following injection of the radioligand. Source organs were identified at each time point from planar images.

**Results** The peak activities in planar images in the six identified source organs (expressed as per cent injected dose (%ID)) were lungs (16.5%ID at 2 min), kidneys (12.5%ID at 3 min), brain (9.5%ID at 6 min), liver (7.5%ID at 3 min), red bone marrow (3.5%ID at 12 min), and urinary bladder (2%ID at 98 min). Radiation absorbed doses were calculated using the gastrointestinal tract model in two ways: (1) assuming no urine voiding, and (2) using a dynamic bladder model with voiding intervals of 2.4 and 4.8 h. Using the gastrointestinal tract model and

dynamic bladder model with a voiding interval 4.8 h, the three organs with highest exposure (in  $\mu\text{Gy}\cdot\text{MBq}^{-1}$  ( $\text{mrad}\cdot\text{mCi}^{-1}$ )) were kidneys 75.68 (280), lungs 44.86 (166) and urinary bladder 58.38 (216). Effective doses estimated with and without urine voiding were in the range 21.35–22.70  $\mu\text{Gy}\cdot\text{MBq}^{-1}$  (79–84  $\text{mrad}\cdot\text{mCi}^{-1}$ ).

**Conclusion** The estimated radiation burden of  $^{18}\text{F}$ -FECNT is relatively modest and would allow multiple scans per research subject per year. *Nucl Med Commun* 25:737–742  
© 2004 Lippincott Williams & Wilkins.

Nuclear Medicine Communications 2004, 25:737–742

**Keywords:**  $^{18}\text{F}$ -FECNT, dopamine transporter, dosimetry, whole-body biodistribution, PET, positron emission tomography

Molecular Imaging Branch, National Institute of Mental Health, National Institutes of Health, Bldg 1 Rm. B3-10, 1 Center Drive, Bethesda, MD 20892-0135, USA.

Correspondence to Dr Dnyanesh Tipre, Molecular Imaging Branch, NIMH, Bldg 1, Rm. B3-10, 1 Center Drive, MSC 0135 Bethesda, MD 20892-0135, USA.  
Tel: +1 301 594 1437; fax: +1 301 480 3610;  
e-mail: TipreD@intr.nimh.nih.gov

Received 28 August 2003 Revised 4 January 2004  
Accepted 16 January 2004

## Introduction

The dopamine transporter (DAT) is a carrier protein that transports dopamine across the presynaptic membrane. The DAT terminates the action of dopamine (DA) in the synapse via re-uptake and thus regulates DA neurotransmission. DA plays a vital role in the regulation and control of movement, motivation, and cognition [1,2] and is also closely linked to reward, reinforcement and addiction. Abnormalities in brain DA are associated with many neurological and psychiatric disorders, including Parkinson's disease, schizophrenia, attention deficit hyperactivity disorder, and substance abuse [3–6]. This has made the DA system an important research topic in neuroscience, neuroimaging and drug development [7–9].

Several positron emission tomography (PET) radioligands for DAT are currently available to measure regional DAT levels in brain [10,11]. 2 $\beta$ -Carbomethoxy-3-(4-chlorophenyl)-8-(2-[ $^{18}\text{F}$ ]fluoroethyl)nortropane ( $^{18}\text{F}$ -FECNT) is

one of the best radioligands for this purpose because of its high ratio of DAT-specific to non-displaceable uptake, and also because of its rapid uptake and washout from the brain, characteristics that are highly amenable to kinetic analysis [12].

An important safety consideration in the use of any radioligand is the accurate assessment of the resulting radiation exposure to organs of the body. Radiation dosimetry estimates were recently published for  $^{18}\text{F}$ -FECNT based upon whole-body distribution of radioactivity in rats and monkeys [13] without applying a dynamic bladder model or gastrointestinal (GI) tract model. Cumulative excretion of activity in GI tract and urinary bladder significantly affects radiation exposure to the other organs. Since the dynamic bladder model and GI tract model were not included in the previous study [13], the magnitude of dosimetry errors was unknown. The purpose of the this study was to reassess and

evaluate the biodistribution of  $^{18}\text{F}$ -FECNT activity in rhesus monkeys. Radiation absorbed doses were calculated using the International Commission on Radiological Protection (ICRP) 30 GI tract model either with the assumption of no urine voiding or with a dynamic bladder model (2.4 and 4.8 h).

## Materials and methods

### Radiopharmaceutical preparation

2 $\beta$ -carbomethoxy-3-(4-chlorophenyl)-8-(2-[ $^{18}\text{F}$ ]fluoroethyl) nortropane ( $^{18}\text{F}$ -FECNT) [14,15] was synthesized by alkylation of 2 $\beta$ -carbomethoxy-3 $\beta$ -(4-chlorophenyl)nortropane with 1-[ $^{18}\text{F}$ ]fluoro-2-tosyloxyethane, as previously described [16]. The three doses used for this study were analysed by high-performance liquid chromatography [16] and revealed radiochemical purities of 98.5, 99.8 and 100%, with specific activities of 250.27 GBq  $\mu\text{mol}^{-1}$  ( $\sim 6765$  mCi  $\mu\text{mol}^{-1}$ ) at the time of injection.

### Animals

Three male rhesus monkeys (7, 9 and 12 kg) were initially anaesthetized with ketamine (10 mg  $\text{kg}^{-1}$ ) and subsequently with isoflurane (1.5%) for the duration of each scanning experiment. A urinary catheter was inserted and clamped so that the radioactivity overlaying the bladder represented the total urinary excretion during the scanning interval. The electrocardiograph (ECG), body temperature, heart and respiration rates were measured throughout the experiment.

### PET image acquisition

Whole-body transmission and emission scans were acquired on a GE Advance tomograph (GE Medical Systems, WI). Before injection of the radioligand, each animal received a 40 min whole-body transmission scan from four or five sections of the body from head to mid-thigh for subsequent attenuation correction of the emission image. Two rotating  $^{68}\text{Ge}$  rods were used as the radiation source. Whole-body emission scans were performed following the intravenous administration of 155, 181 and 180 MBq (4.19, 4.90 and 4.87 mCi) of  $^{18}\text{F}$ -FECNT. Serial dynamic images were acquired for a total of 220 min from head to mid-thigh. Each section of the body was imaged 23–30 times, with the following sequence of frame acquisitions: two frames  $\times$  0.25 min, three frames  $\times$  0.50 min, six frames  $\times$  1 min, five frames  $\times$  2 min, seven frames  $\times$  4 min.

### Image and data analysis

The planar image was created by summing the activity values in all overlaying voxels from the 35 horizontal tomographic images in the anterior/posterior direction. Planar images were analysed with PMOD 2.4 (pixel-wise modelling computer software, PMOD Group, Zurich, Switzerland). Urinary bladder, brain, kidneys, liver, lungs, abdomen and vertebra were easily identified on the emission images. However, other organs, including

spleen, thyroid and other bone structures, had inadequate activity to be identified on the emission images. Activity in vertebra and entire abdomen was assumed as red bone marrow and GI tract, respectively. To estimate activities in source organs in a conservative way, a single large region of interest was drawn which included all activity in the organ and overlying tissue as well and some amount from adjacent regions. Activity in 'remainder of body' was calculated at each time point by subtracting that present in the identified source organs from the decayed value of the injected activity.

Activities in the source organs (not decay corrected) were expressed as a percentage of injected dose and plotted versus time. The area under the time-activity curve of each organ was calculated with the trapezoidal method up to the last data acquisition at 220 min. To be conservative, the area under the curve from the last data acquisition (220 min) to infinity was calculated by assuming only physical decay (half-life for  $^{18}\text{F}$  is 109.8 min) and no additional biological clearance. The area under the time-activity curve of source organ from time zero to infinity is equivalent to the residence time (h). The residence times from the monkey were converted into corresponding human values by multiplication with a factor to scale organ and body weights by using the equation  $(b_m/o_m) \times (b_h/o_h)$ , where  $b_m$  and  $b_h$  are the body weights of monkey and human, respectively; and  $o_m$  and  $o_h$  are the organ weights of monkey and human, respectively.

For a conservative estimation, decay corrected peak activity in the entire abdomen, excluding the liver and kidneys, was used as the input to the small intestine in the ICRP 30 GI tract model. This activity contained that outside GI tract, such as activity in muscles and fat tissues. The ICRP 30 GI tract model was implemented in MIRDOSE 3.1 software, and the mean peak excreted activity in the entire abdomen was used as the input to the small intestine to calculate the residence time of the upper large intestine, small intestine and lower large intestine.

The mean cumulative urine activities from three animals were fitted with a bi-exponential curve to estimate the percentage of injected dose excreted via this route. The dynamic bladder model, implemented in MIRDOSE 3.1 software, was applied to calculate the residence time of the urinary activity with voiding intervals of 2.4 and 4.8 h. Organ absorbed doses were based on the MIRD scheme [17] of a 70 kg human subject, using the residence times calculated above with the MIRDOSE 3.1 computer program.

## Results

The injection of  $^{18}\text{F}$ -FECNT with associated carrier ( $\sim 0.76$  nmol) caused no change in ECG, heart or

respiration rates. Recovery of radioactivity from planar images was 84.5, 89.0 and 84.6% of the injected activity in the three monkeys. We calculated radiation absorbed doses by multiplying each organ activity by 100/84.5, 100/89.0 and 100/84.6. Thus, recovered activity was used to calculate the per cent injected dose and residence times of different organs. On the whole-body emission images, urinary bladder, brain, kidneys, liver, lungs, entire abdomen (GI tract) and vertebra were visually identified as organs with moderate to high activity (Fig. 1). In planar images, the peak values of the per cent injected dose to the lungs, kidneys, brain, liver, red bone marrow and urinary bladder were 16.5%, 12.5%, 9.5%, 3.5% and 2% at peak times 2, 3, 6, 3, 12 and 98 min, respectively (Fig. 2). Assuming no urine voiding, the four organs with highest exposures (in  $\mu\text{Gy}\cdot\text{MBq}^{-1}$  (mrad·mCi $^{-1}$ )) were kidneys 75.6 (280), lungs 44.8 (166), upper large intestine 39.7 (147) and urinary bladder 51.8 (192). Assuming a urine voiding interval of 4.8 h the four organs with highest exposures (in  $\mu\text{Gy}\cdot\text{MBq}^{-1}$  (mrad·mCi $^{-1}$ )) were kidneys 75.7 (280), lungs 44.9 (166), upper large intestine 40.0 (147) and urinary bladder 58.4 (216).

The ICRP 30 GI tract model was implemented to calculate the residence time of the upper large intestine, small intestine and lower large intestine. The average per cent excretion of radioactivity in the entire abdomen from three monkeys was 7.5% at a peak time of 12 min (Fig. 3).

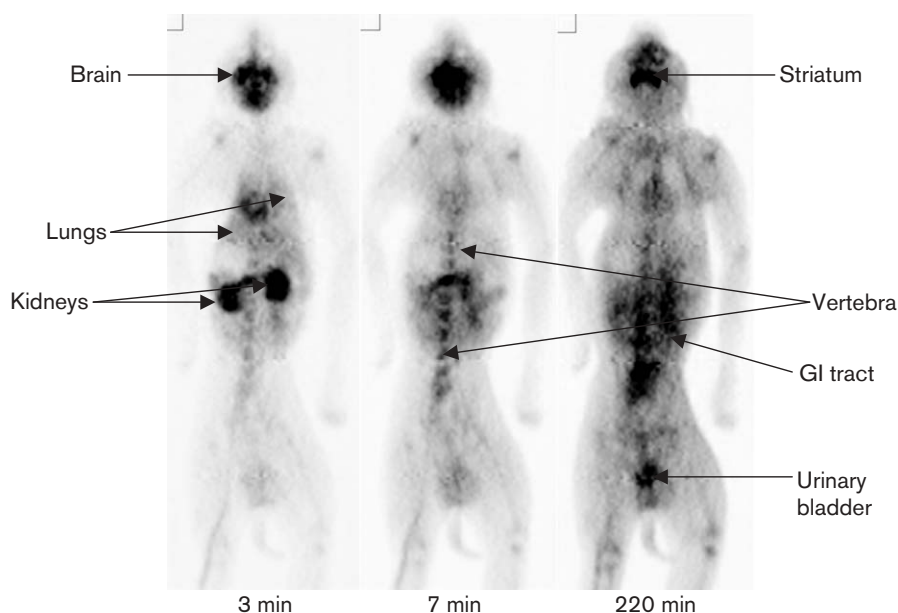
The mean cumulative urinary excretion of  $^{18}\text{F}$ -FECNT was only 7.5% at the end of the study (220 min). This activity was fitted with a bi-exponential association curve (Fig. 4). Fractions of urinary excretion were 1.5% and 98.9% with corresponding biological half-lives of 0.100 and 42.5 h, respectively. Although the goodness of fit was high ( $r^2 = 0.965$ ), the identifiability of parameters was poor. Therefore, residence time of the bladder contents was calculated in two ways: (1) assuming no urine voiding, and (2) using Cloutier's dynamic bladder model [18] with voiding intervals of 2.4 and 4.8 h.

The average residence times for the three animals from planar images are shown in Table 1. From these residence times, radiation absorbed dose estimates were calculated with MIRDOSE 3.1 computer program (Table 2). Effective doses estimated with and without urine voiding were in the range 21.4–22.7  $\mu\text{Gy}\cdot\text{MBq}^{-1}$  (79–84 mrad·mCi $^{-1}$ ).

## Discussion

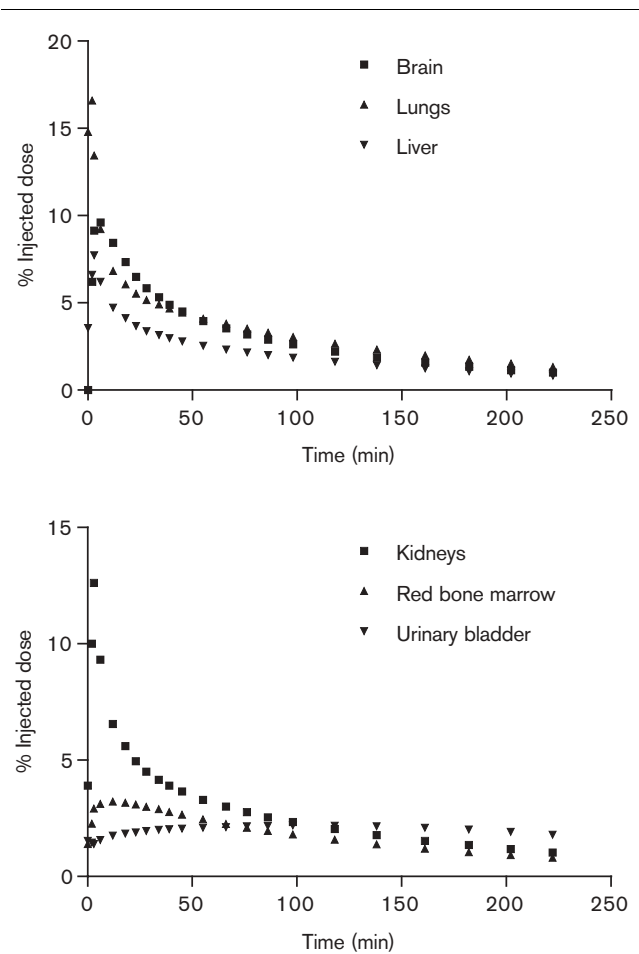
Whole-body imaging of  $^{18}\text{F}$ -FECNT showed that this DAT radioligand caused modest radiation exposure for injected activities (185–370 MBq (5–10 mCi)) commonly used for brain imaging in human subjects. With an effective dose of 0.022 mSv·MBq $^{-1}$  (82 mrem·mCi $^{-1}$ ), these common injected activities of 185–370 MBq would yield an effective dose of 41–82 Sv (410–820 mrem). National, international and local authorities set varying guidelines on radiation exposure for human subjects involved in research studies. Revised guidelines based

Fig. 1



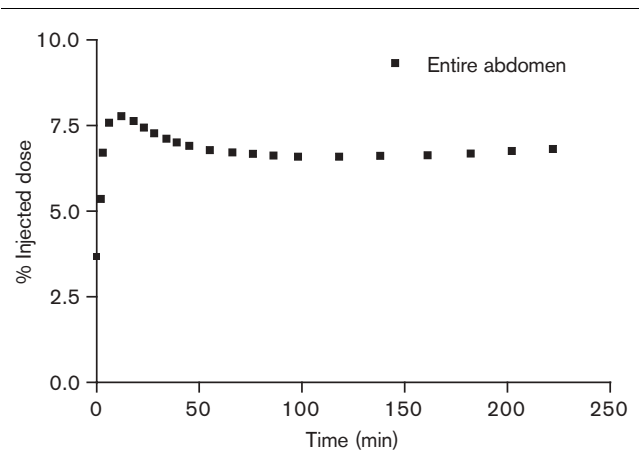
Biodistribution of  $^{18}\text{F}$ -FECNT in monkey #1 at 3, 7 and 220 min after injection. In these planar images, the left side of the animal is on the left side of the image. The highest activities are seen in striatum, kidneys, lungs and abdomen.

Fig. 2



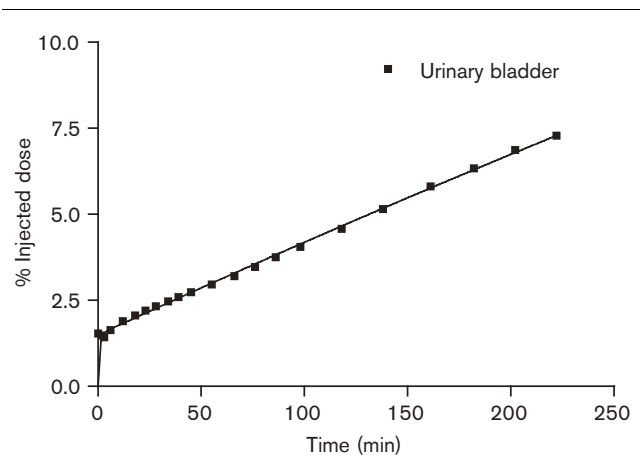
The mean organ uptake over time. The mean time-activity curves (not decay corrected) from the three animals were determined on planar images and expressed as per cent injected dose of  $^{18}\text{F}$ -FECNT.

Fig. 3



The mean time-activity curve (decay corrected) for entire abdomen were determined from the three animals on planar images and expressed as per cent injected dose of  $^{18}\text{F}$ -FECNT.

Fig. 4



Average cumulative urinary excretion of decay corrected activity following intravenous administration of  $^{18}\text{F}$ -FECNT into animals. The curve overlying the measured data points represents a bi-exponential fitting as described in the text.

Table 1 Average residence times for three rhesus monkeys calculated from whole-body planar images

Organ	Residence time (h)
Brain	0.18
Kidneys	0.11
Red bone marrow	0.10
Lungs	0.23
Liver	0.09
Bladder	0.09
Remainder of body	1.41

upon effective dose were recently instituted for the National Institutes of Health (NIH, Bethesda, MD), with the belief that effective dose is the single best measure of radiation risks [19]. Under the NIH Clinical Center guidelines, research subjects (adult volunteer) should receive no more than 0.5 Sv (5 rem) effective dose per year. For  $^{18}\text{F}$ -FECNT, this 0.5 Sv limit corresponds to 2256 MBq ( $\sim 60$  mCi) per subject per year; or a total of about six injections of 370 MBq (10 mCi) each.

Large regions of interest drawn on planar images gave slightly higher dose exposure values and a more conservative estimate of radiation burden. Our calculated effective dose was comparable to the reported effective dose  $15.6 \mu\text{Gy}\cdot\text{MBq}^{-1}$  ( $58.4 \text{ mrad}\cdot\text{mCi}^{-1}$ ) by Deterding *et al.* [13].

A substantial amount of activity was clearly seen in the liver and would likely have been excreted into the small intestine. Doses to the GI tract were also estimated in a conservative way by using activity in the entire abdomen, including overlapping soft tissues, as the input to the small intestine in the ICRP 30 GI tract model.

**Table 2** Estimated human radiation absorbed doses extrapolated from the monkey data

Target organ	Without voiding		Voiding 2.4 h		Voiding 4.8 h	
	mrad·mCi <sup>-1</sup>	μGy·MBq <sup>-1</sup>	Mrad·mCi <sup>-1</sup>	μGy·MBq <sup>-1</sup>	mrad·mCi <sup>-1</sup>	μGy·MBq <sup>-1</sup>
Adrenals	50	13.5	50	13.5	50	13.5
Brain	121	32.7	121	32.7	121	32.7
Breasts	30	8.1	30	8.1	30	8.1
Gallbladder	53	14.3	53	14.3	54	14.6
LLI wall	69	18.6	68	18.4	70	18.9
Small intestine	135	36.4	134	36.2	135	36.5
Stomach	42	11.3	42	11.3	42	11.3
ULI wall	147	39.7	147	39.7	148	40.0
Heart wall	43	11.6	43	11.6	43	11.6
Kidneys	280	75.6	280	75.7	280	75.7
Liver	64	17.3	64	17.3	64	17.3
Lungs	166	44.8	166	44.9	166	44.9
Muscle	35	9.4	35	9.5	35	9.5
Ovaries	56	15.1	55	14.9	57	15.4
Pancreas	48	13.0	48	13.0	48	13.0
Red marrow	61	16.5	61	16.5	61	16.5
Bone surfaces	50	13.5	50	13.5	50	13.5
Skin	26	7.0	26	7.0	26	7.0
Spleen	44	11.9	44	11.9	44	11.9
Testes	32	8.6	31	8.4	32	8.6
Thymus	36	9.7	36	9.7	36	9.7
Thyroid	34	9.2	34	9.2	34	9.2
Urinary bladder	192	51.8	148	40.0	216	58.4
Uterus	57	15.4	54	14.6	59	15.9
Total body	42	11.3	42	11.3	43	11.6
Effective dose equivalent	101	27.3	98	26.5	102	27.6
Effective dose	82	22.1	79	21.3	84	22.7

The injected mass dose ( $\sim 0.76$  nmol) of FECNT produced no pharmacological effects based on ECG, heart rate or respiration rate. Based on these limited physiological measures,  $^{18}\text{F}$ -FECNT appears to be safe from both a pharmacological and radiation perspective [20].

Effective dose estimated with and without urine voiding were in the range of  $21.4\text{--}22.7$   $\mu\text{Gy}\cdot\text{MBq}^{-1}$  ( $79\text{--}84$   $\text{mrad}\cdot\text{mCi}^{-1}$ ), which is close to the published data ( $15.6$   $\mu\text{Gy}\cdot\text{MBq}^{-1}$  ( $58.4$   $\text{mrad}\cdot\text{mCi}^{-1}$ )) by Deterding *et al.* [13]. These differences may due to species difference or methodological discrepancies.

In summary,  $^{18}\text{F}$ -FECNT exhibited a favourable profile of radiation burden that would allow repeated injections for research studies in human subjects. Whole-body imaging in human subjects, especially with direct measurement of serially collected urine samples, would help to more accurately estimate radiation burden to the bladder wall.

## Acknowledgement

We gratefully acknowledge Dr Masanori Ichise and Lisa Coronado (Radiation Safety Branch, NIH), for critical review of the methods and results, and Dr Cyrill Burger for providing PMOD (version 2.4) software.

## References

- Le Moal M, Simon H. Mesocorticolimbic dopaminergic network: functional and regulatory roles. *Physiol Rev* 1991; **71**:155–234.
- Koob GF, Bloom FE. Cellular and molecular mechanisms of drug dependence. *Science* 1988; **242**:715–723.
- Madras BK, Miller GM, Fischman AJ. The dopamine transporter: relevance to attention deficit hyperactivity disorder (ADHD). *Behav Brain Res* 2002; **130**:57–63.
- Volkow ND, Fowler JS, Gatley SJ, Logan J, Wang GJ, Ding YS, Dewey S. PET evaluation of the dopamine system of the human brain. *J Nucl Med* 1996; **37**:1242–1256.
- Jaber M, Jones S, Giros B, Caron MG. The dopamine transporter: a crucial component regulating dopamine transmission. *Mov Disord* 1997; **12**: 629–633.
- Howell LL, Wilcox KM. The dopamine transporter and cocaine medication development: drug self-administration in nonhuman primates. *J Pharmacol Exp Ther* 2001; **298**:1–6.
- Kopin IJ. The pharmacology of Parkinson's disease therapy: an update. *Annu Rev Pharmacol Toxicol* 1993; **33**:467–495.
- Weeks RA, Brooks DJ. Positron emission tomography and central neurotransmitter systems in movement disorders. *Fundam Clin Pharmacol* 1994; **8**:503–517.
- Volkow ND, Fowler JS. Neuropsychiatric disorders: investigation of schizophrenia and substance abuse. *Semin Nucl Med* 1992; **22**: 254–267.
- Halldin C, Gulyas B, Langer O, Farde L. Brain radioligands –state of the art and new trends. *Q J Nucl Med* 2001; **45**:139–152.
- Verhoeff NP. Radiotracer imaging of dopaminergic transmission in neuropsychiatric disorders. *Psychopharmacology (Berlin)* 1999; **147**: 217–249.
- Goodman MM, Kilts CD, Keil R, Shi B, Martarello L, Xing D, *et al.*  $^{18}\text{F}$ -labeled FECNT: a selective radioligand for PET imaging of brain dopamine transporters. *Nucl Med Biol* 2000; **27**:1–12.
- Deterding TA, Votaw JR, Wang CK, Eshima D, Eshima L, Keil R, *et al.* Biodistribution and radiation dosimetry of the dopamine transporter ligand. *J Nucl Med* 2001; **42**:376–381.
- Goodman MM, Kung MP, Kabalka GW, Kung HF, Switzer R. Synthesis and characterization of radioiodinated *N*-(3-iodopropen-1-yl)-2 beta-carbomethoxy-3 beta-(4-chlorophenyl)tropanes: potential dopamine reuptake site imaging agents. *J Med Chem* 1994; **37**:1535–1542.
- Goodman MM, Keil R, Shoup TM, Eshima D, Eshima L, Kilts C, *et al.* Fluorine-18-FPCT: a PET radiotracer for imaging dopamine transporters. *J Nucl Med* 1997; **38**:119–126.

- 16 Chin FT, McCarron JA, Musachio JL, Hong J, Pike VW. A 'ONE-POT' synthesis of [ $^{18}\text{F}$ ]FECNT and its implementation in a commercial automated radiosynthesis apparatus. *J Lab Comp Radiopharm* 2003; **46**:S215.
- 17 Loevinger RBT, Watson EE. *MIRD Primer for Absorbed Dose Calculations*. The Society of Nuclear Medicine, 1991.
- 18 Cloutier RJ, Smith SA, Watson EE, Snyder WS, Warner GG. Dose to the fetus from radionuclides in the bladder. *Health Phys* 1973; **25**:147–161.
- 19 International Commission on Radiological Protection. Radiological Protection and Safety in Medicine. (ICRP Publication 73.) *Annals ICRP* 1996; **26**(1–2).
- 20 Davis MR, Votaw JR, Bremner JD, Byas-Smith MG, Faber TL, Voll RJ, *et al*. Initial human PET imaging studies with the dopamine transporter ligand  $^{18}\text{F}$ -FECNT. *J Nucl Med* 2003; **44**:855–861.